Slow Diffusion Reveals the Intrinsic Electrochemical Activity of Basal Plane Highly Oriented Pyrolytic Graphite Electrodes

ARTICLE *in* THE JOURNAL OF PHYSICAL CHEMISTRY C · MAY 2009

Impact Factor: 4.77 · DOI: 10.1021/jp8092918

3 AUTHORS, INCLUDING:

Martin Andrew Edwards
University of Utah
37 PUBLICATIONS **519** CITATIONS
SEE PROFILE

Paolo Bertoncello
Swansea University
41 PUBLICATIONS **1,263** CITATIONS
SEE PROFILE

Slow Diffusion Reveals the Intrinsic Electrochemical Activity of Basal Plane Highly Oriented Pyrolytic Graphite Electrodes

Martin A. Edwards,[⊥,†,‡] Paolo Bertoncello,[*,⊥,†,§] and Patrick R. Unwin[*,†]

Department of Chemistry, University of Warwick, Coventry CV4 7AL, United Kingdom, and MOAC Doctoral Training Centre, University of Warwick, Coventry CV4 7AL, United Kingdom

Received: October 21, 2008; Revised Manuscript Received: April 4, 2009

This paper reports a method for distinguishing the electroactivity of different types of sites on heterogeneous electrode surfaces, exemplified through studies of basal plane highly oriented pyrolytic graphite (HOPG) electrodes. By depositing a thin film of Nafion with incorporated redox species (i.e., tris(2-2′-bipyridyl)ruthenium(II), $Ru(bpy)_3^{2+}$, and hexaaminoruthenium(III), $[Ru(NH_3)_6]^{3+}$) onto HOPG, diffusion is greatly slowed down. On the time scale of cyclic voltammetry, one can then distinguish between different scenarios of electrode activity because sites on the electrode, with different activity, become diffusionally decoupled. In particular, we show that one can discriminate readily between limiting cases in which the basal plane of HOPG is considered to be either (i) completely active or (ii) inert (with only step edges active). Experimental measurements coupled to modeling show unequivocally that the basal plane of HOPG is electrochemically active. The methodology described and the results obtained have important implications for understanding the intrinsic activity of the basal plane and step edges of graphite electrodes and related carbon-based electrode materials.

Introduction

A large number of reports have appeared over several decades focusing on the electrochemical properties and applications of carbon-based materials.[1−13] Because of their widespread use in electroanalysis, there has been particular interest in understanding the factors influencing electron transfer (ET) kinetics at such electrodes.[1,9−11,14−17] Many fundamental studies have considered basal plane highly oriented pyrolytic graphite (HOPG) because of the possibility of forming well-defined surfaces over extended length scales. Largely on the basis of cyclic voltammetry (CV) measurements, consensus is that basal plane HOPG appears to have rather slow ET kinetics for a range of redox couples, in contrast to edge plane HOPG,[9,11,15,16,18−20] although it is also recognized that the activity of basal plane HOPG is dependent on the redox couple and electrode history.[1] More recently, it has been reported that the ET rate constant for the ferro-/ferricyanide couple at basal plane HOPG is essentially zero and that step edges alone are responsible for the voltammetric response.[12,13,21−23] This interpretation has also been extended to different classes of carbon-based materials, such as carbon nanotubes (CNTs).[12,13,24] For example, it has been suggested that the electrocatalytic activity of multiwalled carbon nanotubes (MWNTs) resides in ET from the ends of nanotubes and at step edges,[12,13] but in some work, the electrochemical response of single-walled carbon nanotubes (SWNTs) has been attributed to the metal nanoparticles from which they are grown.[24b] These observations contrast with other work on well-defined SWNT samples that indicate that the basal sidewalls have considerable activity.[25−30] Attempts to examine the effects of defects on the electrochemistry of HOPG surfaces have included laser activation[19] and electrochemical pretreatment[20] to deliberately alter the surface structure.

A complication in the interpretation of the ET rates at heterogeneously active electrodes is diffusional overlap between sites of different activity on the characteristic voltammetric time scale. The proposition in this paper is that by slowing diffusion, sites with different activity become decoupled so that one can obtain new insights into the reactivity. In particular, we are able to discriminate easily between the limiting cases when HOPG activity is due to (i) only step edges and (ii) the basal (and step edges). Our work clearly shows that the basal plane of HOPG has intrinsic ET activity. To slow diffusion to HOPG, we use a Nafion coating. Nafion is a perfluorinated ionomer widely used in electroanalysis because of its excellent ion-exchange and permselectivity properties.[31] Nafion is characterized by a multiphase structure consisting of fluorocarbon hydrophobic phases, hydrophilic sulfonated ionic clusters and interfacial regions[21−23,32] that can be loaded with cationic redox species.[31,33−39] Anion-selective coatings could be used in a similar way, to the studies herein, to examine the ET activity of anionic redox species at HOPG.

We have recently reported on the electrochemical properties of redox mediators loaded in ultrathin Nafion Langmuir−Schaefer (LS) films[33,34] deposited on indium tin oxide electrodes, as well as a novel procedure to incorporate redox mediators directly into Langmuir monolayers.[35,36] The distribution of redox species in LS films of this type has recently been shown to be reasonably homogeneous.[40] The compactness of the Nafion LS films significantly decreases the apparent diffusion coefficients of the loaded redox species.[33,36] In this study, the encapsulation of the outer-sphere redox species, tris(2-2′-bipyridyl)(ruthenium(II), $(Ru(bpy)_3^{2+/3+})$ and $[Ru(NH_3)_6]^{3+/2+}$, allows us to assess the intrinsic electrochemical activity of the basal plane of HOPG toward these couples.

* Corresponding authors. E-mails: p.r.unwin@warwick.ac.uk (P.R.U.), paolo.bertoncello@dcu.ie (P.B.).
⊥ These authors contributed equally to the work.
† Department of Chemistry.
‡ MOAC Doctoral Training Centre.
§ Present address: Biomedical Diagnostics Institute, Dublin City University, Glasnevin, Dublin 9, Ireland.

10.1021/jp8092918 CCC: $40.75
Published on Web 04/29/2009

Past work indicates that $Ru(bpy)_3^{2+/3+}$ and $[Ru(NH_3)_6]^{3+/2+}$ display quasi-reversible kinetics at basal plane HOPG on the CV time scale.[1] Since both couples show very rapid ET on a range of other electrode materials,[1] one might explain this behavior using a model similar to that proposed for ferro-/ferricyanide in which only adventitious step edges are highly active and the basal plane is essentially inactive.[12,13,24] The methodology herein allows this proposition to be tested. The results of CV experiments, supported by finite element method simulations, provide unequivocal evidence that a significant portion of the electrochemical activity of HOPG electrodes resides with the basal plane itself.

Experimental Section

Materials. Nafion 117 solution (5% w/v mixture of low molecular weight alcohols), sodium chloride, and tris(2-2′-bipyridyl)ruthenium(II), ($Ru(bpy)_3^{2+}$) dichloride salt, were purchased from Sigma-Aldrich. Hexaamminoruthenium(III) trichloride was purchased from Strem Chemicals. All other chemicals were of reagent grade quality and used as received.

HOPG (SPI-1 grade), 10 mm × 10 mm × 2 mm was purchased from SPI Supplies, West Chester, PA was used for electrochemical experiments. This was used for the present studies to allow direct comparison with recent solution phase work.[12,13] Freshly prepared HOPG surfaces were obtained by cleaving using adhesive tape. Tapping mode AFM topographical analysis revealed well-defined basal plane surfaces with parallel steps with characteristic spacing typically in the range 0.5−1.0 μm, although occasionally, step spacings as close as 0.2 μm were observed. Typical AFM images on the related ZYA grade material, which has a slightly lower density of steps, have been reported recently.[41] All aqueous solutions were prepared from Milli-Q reagent water (Millipore Corp.), resistivity ≥18.2 MΩ cm at 25 °C.

Fabrication of Nafion Langmuir−Schaefer Films. Nafion LS films containing either $Ru(bpy)_3^{2+}$ or $[Ru(NH_3)_6]^{3+}$ were deposited onto HOPG electrodes using a well-established procedure reported by us.[35,36] A Langmuir trough (total volume 1 L, from Nima Instruments, Coventry, UK) was used in which the surface pressure was measured by means of a Wilhemy balance with an accuracy of ±0.1 mN m^{-1}. The volume of Nafion−$Ru(bpy)_3^{2+}$ and Nafion−$[Ru(NH_3)_6]^{3+}$ added to the subphase (initial area 489 cm^2) was, in all cases, 200 μL. A 2 min period was allowed to elapse before compression of the floating films. On the basis of our previous reports,[35,36] the fabrication of Nafion−$Ru(bpy)_3^{2+}$ and Nafion−$[Ru(NH_3)_6]^{3+}$ films utilized a surface pressure of 20 mN m^{-1} and 0.1 M of NaCl as the subphase. Films were built up in a layer-by-layer fashion and in this work were typically 90 (±10) nm thick (comprising 50 layers).

Electrochemistry. CV measurements were made using an electrochemical analyzer (CH Instruments, model CHI730A). We used a setup in which a droplet of electrolyte solution (10 μL) was deposited on the sample,[30] comprising HOPG modified with an ultrathin film of Nafion, deposited as described above. There were no issues with evaporation on the time scale of the measurements. A three electrode configuration was used in which the working electrode was modified basal plane HOPG. A platinum gauze was used as a counter electrode, and a Ag wire served as a quasi-reference electrode (AgQRE). The area of the surface covered by the solution was typically 0.15 (±0.015) cm^2, and this was measured using a video microscope.

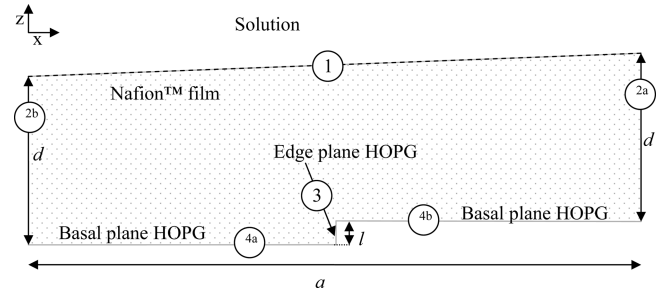

Figure 1. Schematic of the geometry used for the simulation. The size of the step edge is exaggerated for clarity. Circled numbers are indicative of the boundary conditions defined in the text.

TABLE 1: Summary of the Values of Physical Parameters Used in the Finite Element Simulation of CVs of Nafion-Functionalized LS Films

redox couple	surface coverage (Γ)/10^{-10} mol cm^{-2}	D_{app}/10^{-11} cm^2 s^{-1}	c_b/mol dm^{-3}
$[Ru(NH_3)_6]^{3+/2+}$	33	12.0	0.41
$Ru(bpy)_3^{2+/3+}$	46	4.7	0.51

All voltammetric data are presented as current density, with the current normalized by the area of the substrate electrode covered by solution.

Finite Element Modeling. Numerical simulations were performed on a Viglen Intel Core 2 Duo 2.4 GHz computer equipped with 4 GB of RAM and running Windows XP 64 bit edition. Modeling was performed using the commercial finite element modeling package Comsol Multiphysics 3.3a (Comsol AB, Sweden), using the Matlab interface (Release 2006b) (MathWorks Inc., Cambridge, UK). Simulations were carried out with >30 000 triangular mesh elements. Mesh resolution was defined to be greatest around the step edge on the surface (see below). Simulations with finer meshes were completed (not reported) to confirm the mesh sufficiently fine as to not adversely affect the accuracy of the solution.

It is assumed that no transfer of electroactive species takes place at the film−solution interface. This assumption is valid on the time scale of the measurements performed and was verified by the reproducibility of sequential voltammetric measurements on the same film.

Theory and Simulations

The following system is considered: an ultrathin Nafion film containing a redox mediator ($Ru(bpy)_3^{2+}$ or $[Ru(NH_3)_6]^{3+}$) deposited on an HOPG electrode. We define the model for the reduction of $[Ru(NH_3)_6]^{3+}$; however, recasting for the oxidation is trivial. We seek a description of the concentration of $[Ru(NH_3)_6]^{3+}$ within Nafion LS films and the current response as a function of applied potential: this is achieved through the solution of the time-dependent version of the diffusion equation (eq 1).

$$\frac{\partial c}{\partial t} = D_{app}\nabla^2 c \qquad (1)$$

where c represents the concentration of $[Ru(NH_3)_6]^{3+}$ and D_{app} represents its apparent diffusion coefficient, which may include some contribution from electron hopping.[31,42−44] The apparent diffusion coefficient values of the oxidized and reduced forms of the redox couple were assumed to be equal; hence, the concentration of $[Ru(NH_3)_6]^{2+}$ can be represented by ($c_b - c$), where c_b represents the initial concentration of $[Ru(NH_3)_6]^{3+}$. The model makes the assumption that the HOPG step edges

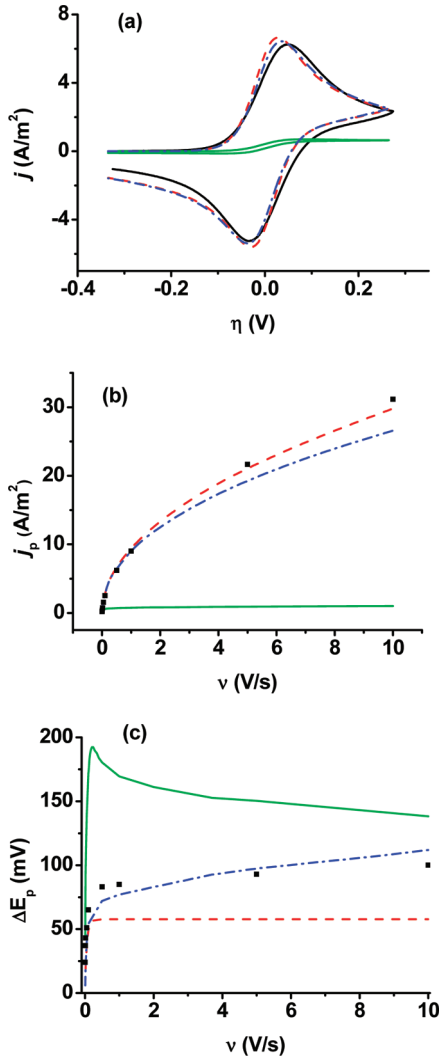

Figure 2. (a) CV of a Nafion−$Ru(bpy)_3^{2+}$ film at a scan rate of 0.5 V s^{-1}. Black line: experimental data. Finite element simulations with basal plane kinetics either reversible (red line), inert (k_0= 0 cm s^{-1} green line), or active with a rate constant of k_0= 1×10^{-4} cm s^{-1} (blue line). (b) Peak current density of the forward potential sweep (j_p) versus scan rate. Squares indicate experimentally recorded data. Lines are from simulated CVs; colors as in part (a). (c) Difference in potential between the forward and reverse sweeps (ΔE_P). Lines and points as in part (b).

run parallel to each other and are equally sized and spaced. We use l and a to represent the step height and distance between the steps on HOPG, respectively. For the simulations presented in this paper, we use values of $l = 2$ nm, and $a = 200$ nm on the basis of the largest and smallest values, respectively, reported in the work of McCreery and co-workers.[9] The use of values away from these extrema are discussed. Note that these values serve as a best case scenario in terms of maximizing the contribution from edge plane sites and, thus, provide the most stringent test of the proposition that step edges alone are responsible for the electrochemical activity of basal plane HOPG.

The surface under consideration is composed of two separate domains (basal plane and edge plane sites). The repeat unit periodic two-dimensional domain is illustrated in Figure 1, with the boundary conditions as follows. At the basal plane sites (Figure 1, edges 4a and 4b), we describe the flux of $[Ru(NH_3)_6]^{3+}$ normal to the surface by

$$D_{app}\frac{\partial c}{\partial z} = k_f c - k_b(c_b - c) \qquad \text{for } z = 0, 0 \le x \le a/2, \text{ and } z = l, a/2 \le x \le a \quad (2)$$

where k_b and k_f are the back and forward rate constants, respectively, for the reaction

$$[Ru(NH_3)_6]^{3+} + e^- \underset{k_b}{\overset{k_f}{\rightleftharpoons}} [Ru(NH_3)_6]^{2+}$$

defined as

$$k_b = k_0 \exp((1 - \alpha)F\eta/RT) \quad (3)$$

$$k_f = k_0 \exp(-\alpha F\eta/RT) \quad (4)$$

where k_0 is the standard rate constant and $\alpha = 0.5$ is the transfer coefficient. $F = 96\,485$ C mol^{-1}, $R = 8.314\,47$ J K^{-1} mol^{-1}, and $T = 298$ K, are, respectively, the Faraday constant, the molar gas constant, and the temperature. $\eta(t) = \eta_0(t) - E^{0\prime}$ is the overpotential at time, t, where $E^{0\prime}$ is the formal electrode potential, and $\eta_0(t)$ is the applied potential, defined as

$$\eta_0(t) = \begin{cases} E_{upper} - \nu t & 0 \le t \le t_1 \\ E_{lower} + \nu(t - t_1) & t_1 < t \le 2t_1 \end{cases} \quad (5)$$

with ν defined as the scan rate; E_{lower} and E_{upper} are the lower and upper limits of the potential range, and $t_1 = (E_{upper} - E_{lower})/\nu$.

At the edge plane sites (Figure 1, edge 3), we ascribe reversible kinetics by setting the concentration,

$$c = \frac{c_b}{1 + \theta} \qquad \text{for } x = a/2, 0 < z < l \quad (6)$$

with

$$\theta(t) = \exp(-\eta(t)\, F/RT) \quad (7)$$

Thus, the reaction is considered to proceed as fast as possible on these sites, again representing a best case scenario in terms of maximizing the contribution of edge sites to the overall current response.

On the periodic boundaries (Figure 1, edges 2a and 2b) we set:

$$c(x = 0, z, t) = c(x = a, z + l, t) \qquad \text{for } 0 < z < d \text{ and } 0 \le t \le 2t_1 \quad (8)$$

At the film−solution interface (Figure 1, edge 1) we define

$$\underline{n}\cdot\nabla c = 0 \qquad \text{for } 0 \le x \le a, z = d + xl/a \quad (9)$$

where $\underline{n}$ represents the inward pointing unit normal vector.

The concentration at time $t = 0$ is taken to be the equilibrium concentration at $\eta(0)$; that is,

$$c_{t=0} = \frac{c_b}{1 + \theta(0)} \quad (10)$$

We calculate the current density by integrating the flux over the HOPG surface (edges 3, 4a, and 4b in Figure 1) divided by the size of the domain simulated.

$$j = \frac{1}{a}FD_{app}\int \underline{n}\nabla c \quad (11)$$

Results and Discussion

The surface coverage of redox species, concentration of redox mediators within the film, film thickness, and apparent diffusion coefficients were extracted from cyclic voltammetric data. The surface coverage, Γ, was determined by integration of the anodic ($Ru(bpy)_3^{2+}$ oxidation to $Ru(bpy)_3^{3+}$) or cathodic ($[Ru(NH_3)_6]^{3+}$

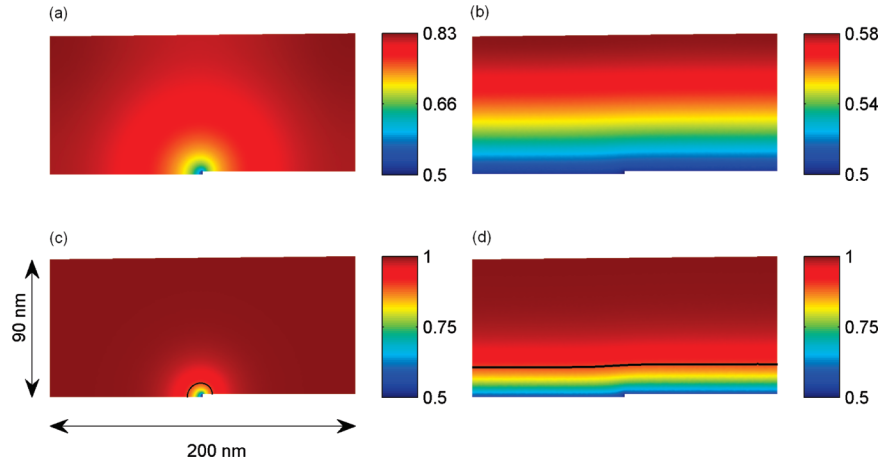

Figure 3. Plots of normalized concentration of reactant at the half-wave potential of a cyclic voltammogram calculated by finite element simulations for a Nafion−$Ru(bpy)_3^{2+}$ film; scan rate (a, b) 10 mV s^{-1}, (c, d) 1 V s^{-1}. Basal plane activity is defined by k_0= 0 cm s^{-1} (a, c) and k_0= 1 × 10^{-4} cm s^{-1} (b, d). The contours plotted in c and d are isoconcentration lines for c = 0.9. Note: concentration scales differ between the images.

reduction to $[Ru(NH_3)_6]^{2+}$) currents for those responses that displayed thin layer, exhaustive electrolysis characteristics (typically at υ = 10 mV s^{-1}).[45] The concentration of the redox species within the film, c_b, was estimated by dividing the values of the surface coverage (Γ, mol cm^{-2}) by the thickness of the film evaluated using AFM in dry conditions. Our previous work has shown swelling of Nafion LS films in solution to be negligible.[35] The measured thicknesses were similar to those Nafion LS films deposited on indium tin oxide (ITO) electrodes:[35] 1.8 and 1.6 nm for Nafion-$(Ru(bpy)_3^{2+}$ and Nafion-$[Ru(NH_3)_6]^{3+}$, respectively.[35] The D_{app} values reported in Table 1 are for 50-layer Nafion LS films and were determined in a manner similar to that for Nafion LS films deposited on ITO electrodes, as reported previously.[35] The values of Γ, c_b, and D_{app} are close to the values determined for Nafion LS films deposited onto ITO electrodes.[35,36]

Figure 2(a) shows a typical experimental CV (scan rate 0.5 V s^{-1}) together with simulated CVs for basal plane kinetics of k_0 = 0, k_0 = 1 × 10^{-4} cm s^{-1} or a fully reversible process. It is clear that the simulated current density with an inert basal plane (step edge only active) is much too low and that a large proportion of the activity observed experimentally must be attributed to ET at the basal plane. Figure 2(b) further illustrates that this assertion holds true over a wide dynamic range, showing the peak current density for the forward sweep as a function of scan rate. The measured peak current density values are very close to those for k_0 = 1 × 10^{-4} cm s^{-1}. However, it is important to note that this closely approximates a reversible process on the basal plane for the time scale of these measurements, particularly given the assumptions about mass transport in the Nafion film, discussed further below. The significant point is that these measurements show that the basal plane of HOPG has considerable electroactivity. The case with the inert basal plane (k_0 = 0 cm s^{-1}) predicts current densities that are much too low. This effect is most evident at the shortest time scales (i.e. higher scan rates (υ > 1 V s^{-1})), where the cases of active and inactive basal plane become most clearly differentiated. For υ = 10 V s^{-1}, the peak current density calculated assuming an inert basal plane is more than 30 times lower than that observed experimentally. Furthermore, as noted above, the simulations in which only the step edge is active have considered the maximum step density possible. In practice, the step density may be lower, and if only the steps were active, one would expect to observe an even lower current response than shown for the inert basal plane case.

Figure 2(c) illustrates how the peak separation between the forward and reverse sweeps varies with sweep rate. It is apparent that the experimentally observed peak separation is significantly less than one would expect with an inert basal plane, but instead matches closely that of an active basal plane. The fit appears closest to k_0 = 1 × 10^{-4} cm s^{-1}, rather than entirely reversible, but resistance may influence these experiments, given the high concentrations of redox-active species in a rather compact film. The quoted value of k_0 should be taken as a lower limit; the value could be significantly higher because the CV measurements could be impacted by film resistance effects, for example. The important point is that all the data in Figure 2, and particularly the peak current data, highlight that the basal plane of HOPG has significant electrochemical activity and cannot be considered to be inactive.

Figure 3 shows simulated normalized concentrations of the redox-active reactant at the half-wave potential on the forward sweep for the situation when the basal plane is inert (Figure 3 (a, c)) and when it is considered as active (k_0 = 1 × 10^{-4} cm s^{-1}) (Figure 3(b, d)) at two different scan rates, 10 mV s^{-1} (a, b) and 1 V s^{-1} (c, d). The other simulation parameters used were those already defined for $Ru(bpy)_3^{2+}$(see Table 1). In the case of an inactive basal plane, mass transport to the step edge is sufficient only to deplete the redox active species in a small zone about the step edge. This is in contrast to the active basal plane case in which a large portion of the film, across almost the entire film thickness at low scan rate, is depleted. Because the rate of depletion is proportional to the current, it is clear why the methodology described is so revealing of the extent of basal plane activity. At faster scan rates, the difference in depletion is accentuated further, which explains the fact that higher scan rates offer more discrimination between the extreme cases in which the basal plane is considered to be either electrochemically active or inactive.

In a way similar to that for the Nafion-$Ru(bpy)_3^{2+}$ films described above, we considered a second system based on Nafion−$[Ru(NH_3)_6]^{3+}$ LS films (Figure 4). A typical experimental CV shown in Figure 4(a) (scan rate 0.5 V s^{-1}) again indicates that the basal plane of HOPG has considerable electrode activity. The simulation of the case in which step edges alone are active predicts current densities that are much too low. This is more evident by examining the forward peak current density over the full range of scan rates (Figures 4 (b)).

The peak−peak separation (ΔE_P) is less diagnostic of basal plane activity but, nonetheless, provides convincing evidence

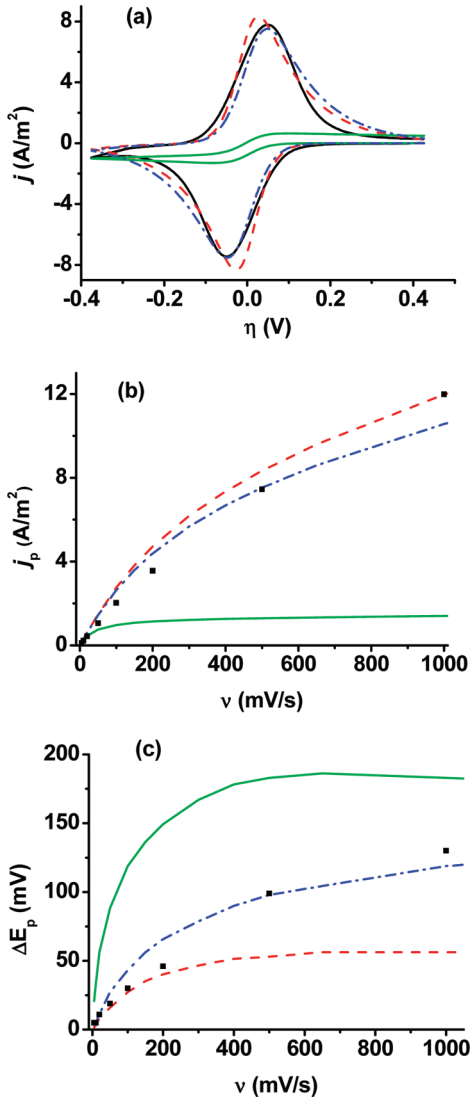

Figure 4. (a) CV of a Nafion−$[Ru(NH_3)_6]^{3+}$ film at a scan rate of 0.5 V s^{-1}. Black line: experimental data. Finite element simulations with basal plane kinetics either reversible (red line), inert (k_0= 0 cm s^{-1}, green line), or active with a rate constant of k_0= 4.5 × 10^{-5} cm s^{-1} (blue line). (b) Plot of peak current density of the forward potential sweep versus scan rate. Squares indicate experimentally recorded currents. Lines are from simulated CVs, colors as in part (a). (c) Plot of the difference in potential between the forward and reverse sweeps (ΔE_P). Lines and points as in part (b).

that supports the peak current analysis. At low scan rates, the peak−peak separation is consistent with reversible ET, but at high scan rates, there is an increase in ΔE_P that matches k_0 = 4.5 × 10^{-5} cm s^{-1} most closely. For the reasons discussed below, this should be taken strictly as a minimum value. The important aspect, again, is that this methodology reveals the basal plane of HOPG to be electrochemically active.

It is important to comment on the rate constants extracted from this analysis. Various factors not included explicitly in the model may have some effect on the peak positions. For example, resistance effects, migration, mixed physical diffusion/electron hopping contributions to the apparent diffusion coefficient. Furthermore, at the highest scan rates, the diffusion layer becomes so thin that heterogeneities in film structure and the interaction of the film with the electrode may become important. These issues lead to some uncertainty in the k_0 values quoted. However, they do not impact the main conclusion of this study that the basal plane of HOPG is highly electroactive and the response closely approximates reversible ET, certainly at scan rates of 200 mV s^{-1} or lower.

As already briefly highlighted, further evidence supporting the deduction that basal plane activity contributes significantly to the overall current response of HOPG electrode surfaces is provided by noting that the step height and spacing used in the simulations were taken to be upper and lower limits, respectively (2 and 200 nm), of those reported and by the fact that kinetics on the step edge were taken to be reversible, thus maximizing their contribution to the current. It is therefore evident that the basal plane must contribute substantially to the net current measured. Additional simulations were performed with lower activity on the step edge, a smaller step height, and wider step spacing (data not shown). These parameters did not significantly alter the CVs where the basal plane was taken to be active but significantly lowered the simulated current density for the inert basal plane case. Because the step edges did not significantly alter the CVs for the active basal plane case, we can conclude that the HOPG basal plane dominates the response seen in our experiments.

It is worth briefly speculating on why other studies[12,13,21−23] have found HOPG to be less active than reported herein. A significant issue is the extensive reliance on ferro-/ferricyanide as a probe redox couple, which does not behave ideally. The source, preparation, characterization, and history of the HOPG material is an additional major issue. Recent high-resolution electrochemical studies from our group[41] and further investigations to be reported in due course[46] show that the HOPG basal plane is highly active for the ferro-/ferricyanide couple, provided the HOPG sample is freshly prepared, but the response deteriorates with time.[46] Metal nucleation studies[47] are often quoted to support the idea that the step edges on HOPG are much more active electrochemically than the basal plane (which may be the case and does not run counter to any of the deductions herein, although definitive *direct* evidence remains to be found). However, whether the results of such studies, which involve much more complex electrochemical nucleation and growth processes (which will naturally be promoted at surface steps), can be translated to outer-sphere electron transfer is questionable. In any case, metal electrodeposition studies[47] clearly show that nucleation and growth occurs at the basal plane of HOPG (albeit less extensively than at step edges).

Conclusions

The use of ultrathin films of Nafion-encapsulated redox species has allowed sufficiently slow diffusional time scales to be accessed such that the intrinsic ET activity of basal plane HOPG can be elucidated unequivocally. Our results show that simple redox couples, such as $Ru(bpy)_3^{2+}$ and $[Ru(NH_3)_6]^{3+}$, undergo close to reversible ET at basal plane HOPG on the time scales considered. Had only the step edges on the basal plane been active, then currents would have been 1−2 orders of magnitude smaller than observed experimentally. It is important to note that if there are variations in activity across the basal plane itself (e.g., point defects) this will have to be on a small length scale to account for the CV observations.

To simplify modeling, mass transport in the film was described solely by diffusion (eq 1) with the apparent diffusion coefficient taken as uniform throughout the film. Migration and electron hopping were not explicitly taken into account. The experimentally determined values for D_{app} will encompass these processes in some sense. However, mass transport in the layer closest to the electrode may differ from that further away due to the influence of the HOPG surface on the carbon/film

interface. There may also be film resistance effects, These points may explain some of the variation seen in the voltammetric analysis of peak potentials at high scan rates but does not impact the most important conclusion about the activity of basal plane HOPG. Rate constants extracted from the analysis will necessarily represent lower limits, and the values reported could be significantly higher.

We are developing complementary methods to provide further insight into the activity of HOPG and other carbon-based materials. Some of the results of these studies have been presented elsewhere,[41] and further reports will follow.[46]

Acknowledgment. This work was supported by a Marie Curie Intra-European Fellowship (P.B. fellowship, MEIF-CT-2005-515356) and COST D36/005/06 within the 6th European Community Framework Programme. MAE was supported by EPSRC (Warwick MOAC Doctoral Training Centre). The support of the EPSRC (EP/D000165/1) is gratefully acknowledged.

References and Notes

(1) McCreery, R. L. *Chem. Rev.* **2008**, *108*, 2646, and references therein.
(2) Uslu, B.; Ozkan, S. A. *Anal. Lett.* **2007**, *40*, 817.
(3) Lee, J.; Kim, J.; Hyeon, T. *Adv. Mater.* **2007**, *18*, 2073.
(4) Guldi, D. M.; Rahman, G. M. A.; Sgobba, V.; Ehli, C. *Chem. Rev.* **2006**, *35*, 471.
(5) Gong, K.; Yan, Y.; Zhang, M.; Su, L.; Xiong, S.; Mao, L. *Anal. Sci.* **2005**, *21*, 1383.
(6) Wang, J. *Electroanalysis* **2005**, *17*, 7.
(7) Svancara, I.; Vytras, K.; Barek, J.; Zima, J. *Crit. Rev. Anal. Chem.* **2001**, *31*, 311.
(8) Flandrois, S.; Simon, B. *Carbon* **1999**, *37*, 2.
(9) Robinson, R. S.; Sternitzke, K. D.; McDermott, M. T.; McCreery, R. L. *J. Electrochem. Soc.* **1991**, *138*, 2412.
(10) McDermott, C. A.; Kneten, K.; McCreery, R. L. *J. Electrochem. Soc.* **1993**, *140*, 2593.
(11) Bowling, R. J.; Packard, R. T.; McCreery, R. L. *J. Am. Chem. Soc.* **1989**, *111*, 1217.
(12) Banks, C. E.; Moore, R. R.; Davies, T. J.; Compton, R. G. *Chem. Commun.* **2004**, 1804.
(13) Banks, C. E.; Davies, T. J.; Wildgoose, G. G.; Compton, R. G. *Chem. Commun.* **2005**, 829.
(14) Rice, R. J.; McCreery, R. L. *Anal. Chem.* **1989**, *61*, 1637.
(15) Kneten, K. R.; McCreery, R. L. *Anal. Chem.* **1992**, *64*, 2518.
(16) Kneten, K. R.; McDermott, M. T.; McCreery, R. L. *J. Phys. Chem.* **1994**, *98*, 5314.
(17) Liu, G.; Freund, M. S. *Langmuir* **2000**, *16*, 283.
(18) Bowling, R.; Packard, R. T.; McCreery, R. L. *Langmuir* **1989**, *5*, 683.
(19) Rice, R. J.; Pontikos, N. M.; McCreery, R. L. *J. Am. Chem. Soc.* **1990**, *112*, 4617.
(20) McCreery, R. L. In *Electroanalytical Chemistry*; Bard, A. J., Ed.; Marcel Dekker: New York, 1991; vol. 17, p 221.
(21) Sternitzke, K. D.; McCreery, R. L. *Anal. Chem.* **1990**, *62*, 1339.
(22) Chen, P.; Fryling, M. A.; McCreery, R. L. *Anal. Chem.* **1995**, *67*, 3115.
(23) Ranganathan, S.; McCreery, R. L. *Anal. Chem.* **2001**, *73*, 893.
(24) (a) Banks, C. E.; Compton, R. G. *Anal. Sci.* **2005**, *21*, 1263. (b) Kruusma, J.; Mould, N.; Jurkschat, K.; Crossley, A.; Banks, C. E. *Electrochem. Commun.* **2007**, *9*, 2330.
(25) Day, T. M.; Unwin, P. R.; Wilson, N. R.; Macpherson, J. V. *J. Am. Chem. Soc.* **2005**, *127*, 10639.
(26) Dumitrescu, I.; Unwin, P. R.; Wilson, N. R.; Macpherson, J. V. *Anal. Chem.* **2008**, *80*, 3598.
(27) Gong, K.; Chakrabarti, S.; Dai, L. *Angew. Chem., Int. Ed.* **2008**, *47*, 5446.
(28) Heller, I.; Kong, J.; Heering, H. A.; Williams, K. A.; Lemay, S. G.; Dekker, C. *Nano Lett.* **2005**, *5*, 137.
(29) Quinn, B. M.; Dekker, C.; Lemay, S. G. *J. Am. Chem. Soc.* **2005**, *127*, 6146.
(30) Bertoncello, P.; Edgeworth, J. P.; Macpherson, J. V.; Unwin, P. R. *J. Am. Chem. Soc.* **2007**, *129*, 10982.
(31) White, H. S.; Leddy, J.; Bard, A. J. *J. Am. Chem. Soc.* **1982**, *104*, 4811.
(32) Mauritz, K. A.; Moore, R. B. *Chem. Rev.* **2004**, *104*, 4535.
(33) Bertoncello, P.; Ciani, I.; Li, F.; Unwin, P. R. *Langmuir* **2006**, *22*, 10380.
(34) Bertoncello, P.; Ciani, I.; Marenduzzo, D.; Unwin, P. R. *J. Phys. Chem. C* **2007**, *111*, 294.
(35) Bertoncello, P.; Wilson, N. R.; Unwin, P. R. *Soft Matter* **2007**, *3*, 1300.
(36) Bertoncello, P.; Dennany, L.; Forster, R. J.; Unwin, P. R. *Anal. Chem.* **2007**, *79*, 7549.
(37) Ugo, P.; Bertoncello, P.; Vezza′, F. *Electrochim. Acta* **2004**, *49*, 3785.
(38) Bertoncello, P.; Ugo, P. *J. Braz. Chem. Soc.* **2003**, *14*, 517.
(39) Bertoncello, P.; Ram, M. K.; Notargiacomo, A.; Ugo, P.; Nicolini, C. *Phys. Chem. Chem. Phys.* **2002**, *4*, 4036.
(40) Moretto, L. M.; Kohls, T.; Chovin, A.; Sojic, N.; Ugo, P. *Langmuir* **2008**, *24*, 6367.
(41) Williams, C. G.; Edwards, M. A.; Colley, A. L.; Macpherson, J. V.; Unwin, P. R. *Anal. Chem.* **2009**, *81*, 2486.
(42) (a) White, H. S.; Leddy, J.; Bard, A. J. *J. Am. Chem. Soc.* **1982**, *104*, 4811. (b) Martin, C. R.; Rubinstein, I.; Bard, A. J. *J. Am. Chem. Soc.* **1982**, *104*, 4817.
(43) Lee, C.; Anson, F. C. *Anal. Chem.* **1992**, *64*, 528.
(44) Anson, F. C.; Blauch, D. N.; Saveant, J. M.; Shu, C.-F. *J. Am. Chem. Soc.* **1991**, *113*, 1922.
(45) Bard, A. J.; Faulkner L. R. *Electrochemical Methods: Fundamentals and Applications*, 2nd ed.; Wiley: New York, 2001, Chapter 6, p 226.
(46) Guille, M.; Patel, A.; O'Connell, M.; Macpherson, J. V.; Unwin, P. R. manuscript in preparation.
(47) Penner, R. M. *J. Phys. Chem. B,* **2002**, *106*, 3339.

JP8092918